

## SEARCH FOR LOW-ENERGY UPSCATTERING OF ULTRACOLD NEUTRONS FROM A BERYLLIUM SURFACE

*Al. Yu. Muzychka, Yu. N. Pokotilovski\**

*Joint Institute for Nuclear Research  
141980, Dubna, Moscow Region, Russia*

*P. Geltenbort*

*Institut Laue-Langevin, Grenoble, France*

Submitted 13 April 1998

We present results of a search for anomalous low-energy upscattering of ultracold neutrons from a beryllium surface. This upscattering is considered one for the possible reasons for UCN «disappearance» from very cold beryllium bottles, as observed in experiments. The indium foil activation method was used to measure a very low intensity flux of upscattered UCN. The (15–300) m/s velocity range of upscattered UCN is ruled out by these measurements at a confidence level of 90%.

### 1. INTRODUCTION

There exists the well-known and long-standing puzzle of ultracold neutron (UCN) storage times in closed volumes, or equivalently, of anomalous losses of UCN upon reflection from the inner surfaces of UCN traps. The most surprisingly large discrepancy between experimental and predicted loss coefficients is observed in the most promising materials for long UCN storage times: cold beryllium [1, 2] and solid oxygen [3]. The anomaly consists of an almost temperature-independent (in the temperature range 10–300 K) wall loss coefficient ( $\sim 3 \cdot 10^{-5}$ ), corresponding to an extrapolated inelastic thermal neutron cross section  $\sigma^* \sim 0.9b$ . This experimental figure for Be is two orders of magnitude higher than the theoretical one, the latter being completely determined at low temperatures by neutron capture in Be (0.008b). The experiment/theory ratio for a very cold oxygen surface reaches three orders of magnitude [3]. Approximate universality of the loss coefficient for beryllium and oxygen, and the temperature independence of the Be figures, forces one to suspect a universal reason for this anomaly.

A series of experiments to find the channel by which UCN leave the trap are described in Ref. 2. None of the suspected reasons has been confirmed: surface contamination by elements with large absorption cross-sections; penetration of UCN through possible micro-cracks in the surface layers of Be; hypothetical milliheating of UCN due to collisions with a low-frequency vibrating surface; upscattering of UCN due to thermal vibrations of the wall nuclei. The latter item deserves special and more careful consideration.

According to the description of the experiment in Ref. 4 (a subsequent conclusion [2] about the absence of UCN upscattering from the beryllium surface at liquid nitrogen temperature is

---

\*E-mail: POKOT@nf.jinr.ru

based entirely on that experiment), upscattered neutrons passed through 1.5 mm of copper, 1.1 mm of stainless steel, and 2 mm of Al prior to entering the neutron detector. For an isotropic distribution of upscattered neutrons, this means that the detection efficiency of upscattered neutrons with energies of 0.5 meV was less than 0.2, and decreased at lower neutron energies. The reported [2] upscattering cross-section of UCN from a beryllium surface at a surface temperature of 80 K was 0.14b with an uncertainty of 30%, so it is quite possible that UCN upscattering takes place to the energy range below 1 meV. This hypothesis is consistent with the observed temperature independence [2] of anomalous losses of UCN if the vibrations causing this upscattering are not thermal in nature. The frequency of these vibrations (possibly surface waves) is in the range  $10^8$ – $10^{12}$  Hz. From a purely experimental point of view (without going into any hypotheses about the reasons for UCN anomalous losses), this low-energy upscattering channel is almost the only one that has not yet been investigated with conclusive results.

Additional qualitative considerations favoring possible high-frequency surface sound wave UCN upscattering comes from the rough coincidence of the typical surface roughness correlation length  $T \sim 300$ – $500$  Å, UCN wavelength  $\lambda$ , which is close to these values, and the possible surface sound wavelength. This coincidence may, in principle, increase the UCN upscattering probability due to some kind of «resonance». If the surface sound velocity  $c \simeq 10^5$  cm/s, then the upscattered neutron energy  $E = hc/\lambda \simeq 10^{-4}$  eV, which is just outside of the investigated energy range [2].

Recently, results have been published [5, 6] describing searches for UCN upscattering from a beryllium foil surface in which gas counters were used for upscattered neutron detection. According to Ref. 5, the total (to the energy range  $(10^{-7} - 10^{-2})$  eV) reduced upscattering cross-section was  $(0 \pm 0.2)$ b at liquid nitrogen temperature, and  $(0 \pm 0.3)$ b at room temperature. The first result is consistent with the early data [2], but the second is in serious disagreement with the previous results. The authors of Ref. 5 point out that these figures are not final, and that «these values were obtained after the subtraction of the large background from the trap walls and separating foil and it is necessary to increase the accuracy of measurements to establish these values».

In contrast, Refs. 6 and 7 give quite different figures for the upscattering loss factor upon UCN reflection from a Be surface:  $(1.47 \pm 0.15) \cdot 10^{-4}$  and  $(1.39 \pm 0.18) \cdot 10^{-4}$  for two different beryllium samples at room temperature, and  $(2.6 \pm 0.3) \cdot 10^{-5}$  and  $(1.7 \pm 0.2) \cdot 10^{-5}$  at liquid nitrogen temperature for the same two beryllium samples.

According to the usual formalism with which UCN interaction with a surface is considered, the UCN reflection probability as a function of the normal component of the neutron momentum  $p_{\perp}$  is

$$w = 2\eta \cdot x / \sqrt{1 - x^2}, \quad x = p_{\perp} / p_{\text{bound}}.$$

The loss factor is

$$\eta = \text{Im } b / \text{Re } b, \quad \text{Im } b = \sigma_{\text{inel}} / 2\lambda,$$

where  $b$  is the coherent scattering length of the wall material,  $p_{\text{bound}} = 2\hbar(\pi Nb)^{1/2}$  is the boundary momentum of the UCN, characterizing the reflecting wall, and  $\sigma_{\text{inel}}$  is the total cross-section of all inelastic UCN interaction processes with the wall surface.

Using the above relations, it is easy to obtain from Refs. 6 and 7 the thermal neutron energy inelastic scattering cross sections for the two beryllium samples,  $\sigma_{\text{inel}} = 2\lambda\eta \text{Re } b$ :  $(4.1 \pm 0.4)$ b and  $(3.9 \pm 0.5)$ b for the room-temperature samples, and  $(0.73 \pm 0.08)$ b and  $(0.48 \pm 0.06)$ b for the liquid nitrogen temperature samples.

It is seen from the above that the results in Refs. 2, 5, 6 and 7 are mutually inconsistent.

For the sake of completeness, it is necessary also to mention measurements [8] of the UCN upscattering probability to the thermal energy range from the surface of a room-temperature beryllium foil after different high-temperature procedures:  $18.5 \cdot 10^{-4}$  before any heating of the sample,  $3.9 \cdot 10^{-4}$  after heating at the  $450^\circ\text{C}$ ,  $4.1 \cdot 10^{-4}$  after heating at  $700^\circ\text{C}$  with subsequent 5-min exposure to atmospheric air, and  $2.2 \cdot 10^{-4}$  after heating at  $700^\circ\text{C}$  in vacuum.

Taking into account that according to Ref. 8 the mean velocity of the stored UCN was measured to be  $\approx 3.2$  m/s, it is possible to transform these figures into the room-temperature neutron upscattering cross-sections if we assume that the imaginary part of the wall potential can be attributed to this cross-section according Eq. (1). This procedure yields for the reduced upscattering cross-sections for the cases mentioned above 76, 16, 17, and 9b respectively, per atom of the wall. These and the previous [2, 5, 6, 7] figures for the reduced upscattering cross-section lead to unrealistically high concentrations of hydrogen in the surface layer of wall if we take into account that the reduced UCN upscattering cross section per hydrogen atom at room temperature is  $\approx (7-8)b$ . It means that the usual procedure that relates the upscattering cross-section to the imaginary part of the wall potential by means of Eq. (1) is incorrect, and can only serve to compare the results of different experiments.

The authors of Ref. 9, which used neutron-induced radiation analysis for the investigation of UCN interaction with beryllium samples, did not find any neutron-capture gamma-radiation from beryllium nuclei. From this fact they concluded that anomalous upscattering with reduced cross-section 0.9b (Gatchina anomaly) can not yield upscattered neutrons with velocity less than  $\sim 70$  m/s in the final state. From this follows a lower bound on the velocity range of the upscattered neutrons:  $v > 70$  m/s (with no indicated confidence level).

## 2. EXPERIMENTAL METHOD

The measurements were performed at the test channel of the UCN turbine source at the Institut Laue-Langevin [10]. The irradiation scheme is shown in Fig. 1.

Ultracold neutrons enter the stainless steel cylindrical chamber 1 ( $\phi = 60$  mm, wall thickness 0.5 mm) through the vertical stainless steel neutron guide 2 (height 120 cm), and rebound from the surface of the specimen 3, made of aluminium foil covered with a beryllium layer (film thickness  $(2-3) \cdot 10^3$  Å). The specimens had the form of a corrugated ribbon rolled into a spiral with an overall area (two sides) of  $\sim 0.5$  m<sup>2</sup> or  $\sim 0.25$  m<sup>2</sup>. The upscattered neutrons leaving the trap penetrate the cylindrical stack of indium foils surrounding the tube and activate them with an activation cross-section that conforms an inverse velocity law. The indium foils were 5–50  $\mu\text{m}$  thick and were manufactured by means of electrolytic deposition on the surface

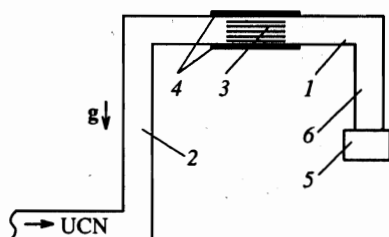


Fig. 1. The layout of an experiment to search for the low-energy upscattering of UCN from a Be surface. 1. Vacuum stainless steel chamber  $\phi 60 \times 0.5$  mm. 2. Vertical UCN guide  $\phi 60 \times 0.5$  mm, height 12 cm. 3. Rouleau of aluminium foils with beryllium deposition. 4. Cylindrical stack of In foils. 5. Detector of UCN ( $^3\text{He}$  proportional counter). 6. Vertical UCN guide  $\phi 60 \times 0.5$  mm, height 60 cm. 7. Shielding (borated polyethylene)

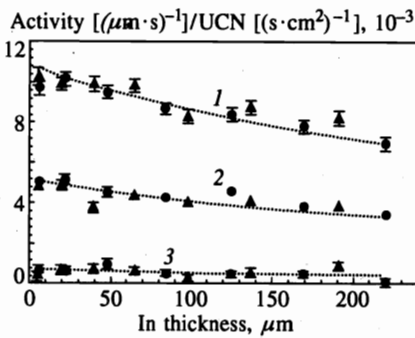


Рис. 2

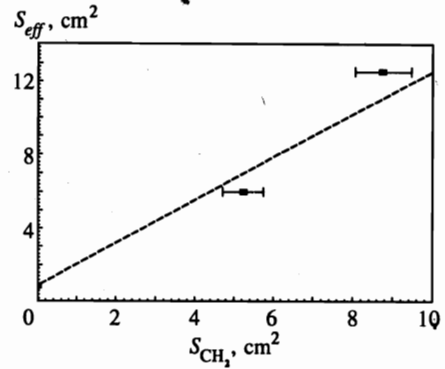


Рис. 3

Fig. 2. Activation of the stack of indium foils as a result of UCN upscattering from polyethylene scatterers with surface area: line 1 —  $8.8 \text{ cm}^2$ ; line 2 —  $5.3 \text{ cm}^2$ ; line 3 — the empty stainless steel chamber

Fig. 3. Measured effective polyethylene sample area obtained from indium foil activation measurements as a function of the polyethylene scatterer surface area

of  $10 \mu\text{m}$  copper foil. The homogeneity of the In thickness was thoroughly verified by cutting the test foils into numerous small specimens and weighing them, and was found to be better than 5%. The density of the UCN flux in the trap was calibrated by means of the activation measurement of the flux of upscattered UCN from small polyethylene samples located at the center of the irradiation chamber, and monitored with a  $^3\text{He}$  proportional counter 5 located after the UCN trap and connected to the trap by a vertical neutron guide 6 through a small ( $0.5 \text{ cm}^2$ ) hole. The UCN flux at the beryllium sample measured in this way was  $\approx 40 \text{ cm}^{-2}\text{s}^{-1}$ .

The efficiency of the UCN detector in the geometry of the experiment was simulated by the Monte Carlo method under various assumptions about the probability of diffuse UCN reflection from the neutron guide walls between the small hole and the membrane of the detector. The results of this simulation show almost constant ( $> 90\%$ ) efficiency in the UCN energy interval of interest, 0–150 neV.

With the known efficiency of the UCN detector it is possible to determine from these measurements the effective areas of the polyethylene samples and to compare them with the actual ones. Figures 2 and 3 show the results of the activation measurements of indium stacks for two polyethylene samples with surface areas of  $5.3$  and  $8.8 \text{ cm}^2$ .

The response function of the activation of the stack of indium foils was calculated by the Monte Carlo method. The upscattered neutrons were assumed to emerge from the Be scatterer isotropically, having their starting points on the surface of the Be spiral. Reflection and absorption of upscattered neutrons along their trajectories were rigorously taken into account.

Detailed results of these simulations will be published elsewhere [11].

Activity of the In foils was measured with a high efficiency ( $\sim 70\%$ )  $4\pi$  scintillation  $\beta$ -counter with active ( $4\pi$  plastic anticoincidence counter) and passive (lead) shielding. The area of the In foils whose activity was measured simultaneously was  $\sim 200 \text{ cm}^2$ . The counter background

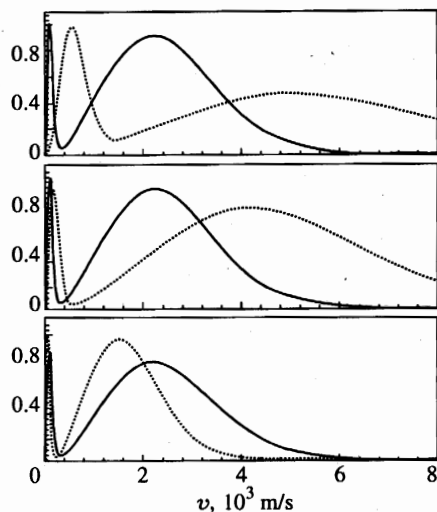


**Fig. 4.** Results of computer indium foil stack «activation experiments» (solid curves) and subsequent restoration of the incoming upscattered neutrons spectra (in relative units) under the assumption that the spectrum consists of two Maxwellian flux components: one with  $v_{th} = 2.2 \cdot 10^5$  cm/s and the other with  $v_0 = 10^4$  cm/s, the latter had a weight 1/20 of the former (dotted curves). The results of computer «activation» of indium foil stack before the restoration procedure were statistically Gaussian distributed with a standard deviation of 5% for each foil

was about  $1.05 \text{ s}^{-1}$  in these measurements. The counter efficiency was carefully measured for different thicknesses of irradiated In and Cu foils. A description of the counter and results of the calibration will be published in Ref. 11.

This method of measuring slow neutron spectra via activation of a stack of In foils was calibrated by irradiating the stack with a beam of monochromatic thermal neutrons or a precisely measured (time-of-flight method) quasi-Maxwellian spectrum of cold and thermal neutrons. The measured and calculated distributions of foil activity along the stacks were in good agreement.

In the absence of low-energy anomalous upscattering, UCN acquire energy from the thermal vibrations of the beryllium lattice, and with higher probability, from vibrations of surface contaminants (mostly hydrogenous). The spectrum of the upscattered neutrons has a «thermal» character, but it is not known. Information about the spectrum of possible «anomalous» upscattering is even more obscure. Therefore, In foil activity measured as a function of position in the stack (thickness coordinate) was approximated under the very general assumption that the spectrum of upscattered neutrons consists of two Maxwellian flux components, one with  $v_{th} = 2.2 \cdot 10^5$  cm/s («normal» upscattering from room temperature Be) and the other with low  $v_0$ , the latter being chosen in the range 10–300 m/s (anomalous upscattering).

The overall thickness of the indium stacks did not exceed  $250 \mu\text{m}$  in our measurements, ( $n\sigma \sim 0.3$  for the isotropic thermal neutron flux), so the accuracy of the upscattered thermal neutron spectrum is not high. But it was demonstrated by rigorous Monte Carlo simulation [11] that it is possible not only to distinguish the low energy component of the upscattering from the high thermal background, but also to carry out rough spectrometry of this low-energy part of the spectrum.

Figure 4 demonstrates some results of the computer indium stack «activation experiment» and restoration of the incoming spectrum of upscattered UCN under the assumption that the spectrum consists of two Maxwellian flux components, one with  $v_0 = 2.2 \cdot 10^5$  cm/s and the second one with  $v_0 = 10^4$  cm/s, the latter had a weight 1/20 of the former.

The results of computer «activation» of the indium foil stack before the restoration procedure were statistically Gaussian-distributed with a standard deviation of 5% for each foil. It can be seen that the method is able to reconstruct with high confidence the small low energy-

admixture to the intensive thermal background, but it is not dependable in extracting the thermal component of the spectrum from the indium activation data.

### 3. RESULTS AND DISCUSSION

Figure 5 shows the measured activity of irradiated In foils as a function of the thickness coordinate for two beryllium samples with different areas.

In our measurements, we used the compact surface sample with the enhanced area, so that the mean gap between the adjacent turns of our helical ribbon sample with area  $\sim 0.5 \text{ m}^2$  was about 1 mm. In UCN upscattering how effectively is the full surface area of the sample used with such narrow channels for UCN diffusion between the adjacent turns? Additional activation measurements were carried out with a sample of area  $\sim 0.2 \text{ m}^2$  with  $\sim 2.5$  times larger gaps between the adjacent turns. Figure 6, representing the measured indium stack activity as a function of sample surface area, shows good proportionality between area and activity, attesting to evidence of the uniform and effective UCN upscattering over the full sample area.

The total measured flux of upscattered UCN from the beryllium sample with area  $0.5 \text{ m}^2$  was  $\sim 50 \text{ s}^{-1}$ .

As mentioned above, this method has low reproducibility in extracting the spectrum of the thermal component of upscattered UCN. Therefore, the experimental data were processed under a different reasonable assumption about the temperature of the thermal component. Figure 7 represents the 90% exclusion contours for the cross-sections  $\sigma_{anom}^*$  and  $\sigma_{th}^*$  deduced from the In foil activation measurement of upscattered UCN fluxes from a normal temperature Be surface, assuming that the thermal component of upscattering represents a Maxwellian neutron flux with room temperature.

The contours are presented for three different characteristic velocities  $v_0$  of anomalously

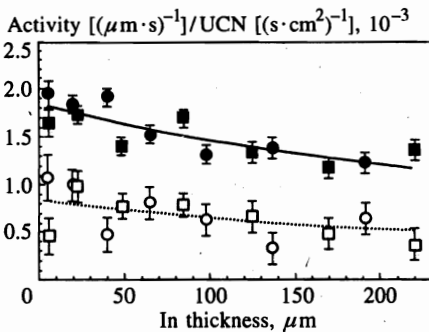


Рис. 5

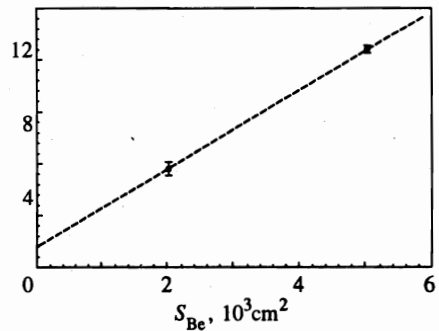


Рис. 6

Fig. 5. Measured In foil activation points as a function of indium thickness coordinate for two different beryllium samples areas: full points  $0.5 \text{ m}^2$ , empty points  $0.2 \text{ m}^2$

Fig. 6. Flux intensity of upscattered UCN normalized per primary UCN flux (relative units) from the beryllium sample as a function of sample area

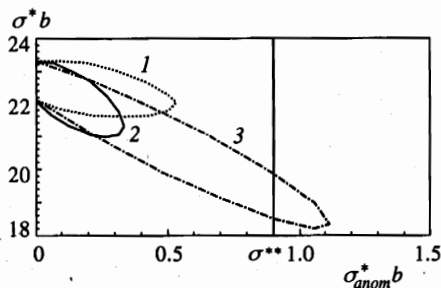


Рис. 7

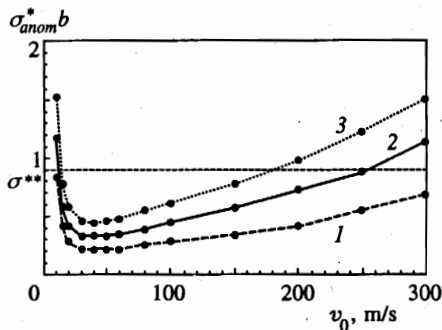


Рис. 8

Fig. 7. The 90% exclusion contours for the cross sections  $\sigma_{anom}^*$  and  $\sigma_{th}^*$  deduced from In foil activation measurement of upscattered UCN flux from normal-temperature Be surface, under the assumption that the thermal component of upscattering represents a Maxwellian neutron flux with room temperature. The contours are presented for three different characteristic velocities  $v_0$  of anomalously (low-energy) upscattered UCN, assumed to have a Maxwellian flux form: line 1 —  $v_0 = 15$  m/s; line 2 —  $v_0 = 50$  m/s; line 3 —  $v_0 = 200$  m/s

Fig. 8. The 90% confidence restriction curves for the reduced cross-section as a function of the characteristic velocity  $v_0$  of the Maxwellian flux of anomalous low-energy UCN upscattering from room-temperature beryllium sample under different assumptions about the characteristic velocity  $v_{th}$  of the thermal flux: line 1 —  $v_{th} = 1600$  m/s; line 2 —  $v_{th} = 2200$  m/s; line 3 —  $v_{th} = 2800$  m/s

(low-energy) upscattered UCN, assumed to have a Maxwellian flux form:  $v_0 = 15$  m/s;  $v_0 = 50$  m/s;  $v_0 = 200$  m/s.

As is seen from Fig. 7 the room-temperature-adjusted UCN upscattering cross-section to the final thermal energy range is very high for non-outgassed beryllium ( $\sim 22b$ ), which is consistent with the result of Ref. 5 and some of the results of Ref. 8. We attribute so large an upscattering cross-section partly to the presence in the incoming UCN spectrum of neutrons with energies higher than the boundary energy of beryllium, but mostly to upscattering from the aluminium cuts of sample ribbons not covered with a beryllium layer. In both cases, this upscattering takes place not at the sample surface but in the bulk of the aluminium. This enhanced thermal upscattering was not very significant in our search for the low-energy anomalous component in the upscattered neutron spectrum, but it increased the thermal background.

Figure 8 shows the 90% confidence restriction curves for the reduced cross-section as a function of the characteristic velocity  $v_0$  of the Maxwellian flux of anomalous low energy UCN upscattering from a room-temperature beryllium sample under various assumptions about the characteristic velocity  $v_{th}$  of the thermal flux.

In addition to (1) the following formulae were used in the data processing. The loss probability of UCN with the velocity  $v$ , averaged over an isotropic angular distribution upon reflection from the surface with boundary velocity  $v_b$ :  $\bar{\mu}_{loss} = 2\eta (\arcsin(y) - y\sqrt{1-y^2})/y^2$ , where  $y = v/v_b$ ,  $\bar{\mu} = \int_0^{v_{lim}} \bar{\mu} f(v) dv$  is the UCN loss coefficient averaged over the normalized UCN flux spectrum  $f(v) = 4v^3/v_{lim}^4$ , which is the low-energy tail of the Maxwellian spectrum. In our case,  $v_{lim} = 3.9$  m/s.

As may be seen from Fig. 8 we were not able to completely rule out in this experiment low-energy UCN upscattering over the entire energy range of interest,  $0.1\text{--}10^3\mu\text{eV}$ , but a significant part of this energy range,  $\simeq (1\text{--}200)\mu\text{eV}$  is ruled out by our measurements.

Preliminary In foil activation measurements with upscattered UCN and partial calibrations of the method in cold and thermal neutron beams were performed at the reactor of the St. Petersburg Nuclear Physics Institute (SPNPI) at Gatchina. We are grateful to Drs. A. P. Serebrov, A. G. Kharitonov, V. V. Nesvizhevsky, and R. R. Taldaev for their kind permission to use the UCN channel of SPNPI and for their very valuable help. We thank them also for placing the Be sample at our disposal. Efficiency measurements of the beta-counter were performed via irradiation of indium and copper foils in the thermal neutron beam of the IBR-2 reactor of FLNP JINR and the microtron neutron source of FLNR JINR. The authors are grateful to Drs. V. V. Nitz and A. G. Belov for their permission to use these installations for our calibrations. We also express our appreciation to the ILL reactor staff.

## References

1. P. Ageron, W. Mampe, and A. I. Kilvington, *Z. Phys. B* **59**, 261 (1985).
2. V. P. Alfimenkov, V. V. Nesvizhevski, A. P. Serebrov et al., LNPI Preprint № 1729, Gatchina, Russia (1991); *Pis'ma v ZETF* **55**, 92 (1992); *JETP Lett.* **55**, 84 (1992).
3. V. P. Alfimenkov, V. V. Nesvizhevski, A. P. Serebrov et al., LNPI Preprint № 1629 (1991), PNPI Preprint № 1756 (1992), Gatchina, Russia.
4. V. K. Ignatovich, Kim Zun Bok, V. I. Lushchikov et al., *JINR Comm. P3-82-811*, Dubna (1982).
5. A. V. Strelkov, G. N. Nekhaev, V. N. Shvetsov et al., in *Neutron Spectroscopy, Nuclear Structure, and Related Topics*, (Proc. IV Int. Seminar on Interaction of Neutrons with Nuclei, Dubna, April 27–30, 1996), p. 299.
6. A. P. Serebrov, in *Neutron Spectroscopy, Nuclear Structure, and Related Topics*, (Proc. V Int. Seminar on Interaction of Neutrons with Nuclei, Dubna, May 14–17, 1997), p. 67.
7. V. E. Varlamov, P. Geltenbort, V. V. Nesvizhevsky et al., Preprint PNPI 2216 Gatchina (1998).
8. L. Bondarenko, S. Chernyavsky, A. Fomin et al., *Physica B* **234–236**, 1189 (1997).
9. S. S. Arzumanov, L. N. Bondarenko, E. I. Korobkina et al., Preprint of Kurchatov Institute IAE-6010/2, Moscow, 1996; S. S. Arzumanov, L. N. Bondarenko, S. M. Chernyavsky et al., Proc. of the Int. Seminar on Interaction of Neutrons with Nuclei ISINN-5: Neutron Spectroscopy, Nuclear Structure, and Related Topics, Dubna, 14–17 May, 1997), p. 91.
10. A. Steyerl, H. Nagel, F.-X. Schreiber et al., *Phys. Lett. A* **116**, 347 (1986).
11. Al. Yu. Muzychka and Yu. N. Pokotilovski, submitted to *Nucl. Instr. Meth.*